Bit Error Rate Analysis of NOMA-OFDM in 5G Systems With Non-Linear HPA With Memory

ALEXANDER HILARIO-TACURI[ID], **JESUS MALDONADO, (Student Member, IEEE),**
MARIO REVOLLO, AND HERNAN CHAMBI
Department of Electronic Engineering, Universidad Nacional de San Agustín de Arequipa, Arequipa 04000, Perú

Corresponding author: Alexander Hilario-Tacuri (ahilariot@unsa.edu.pe)

ABSTRACT The orthogonal frequency division multiplexing (OFDM) and the non-orthogonal multiple access (NOMA) scheme are presented as promising techniques to meet the requirement of fifth-generation (5G) communication systems. Although much attention has recently been devoted to study these techniques, some scenarios have still been less explored. Considering that a fundamental part of any communication system is the use of power amplifiers, this paper presents an analytical evaluation of the bit error rate (BER) of NOMA-OFDM systems in the presence of a high power amplifier (HPA) with memory. Considering that the non-linear distortions generated by the HPA can be modeled using a polynomial model with memory, new theoretical expressions are developed to obtain the BER of the system. Specifically, exact BER expressions for a downlink NOMA-OFDM system with two users are presented and verified by Monte Carlo simulation results. The obtained numerical results demonstrate that the performance degradation of both users is highly dependent on the non-linear distortions, even when the successive interference cancellation (SIC) technique is performed perfectly.

INDEX TERMS 5G, bit error rate, high power amplifier, non-linearity, non-orthogonal multiple access, orthogonal frequency division multiplexing.

I. INTRODUCTION

The Non-Orthogonal Multiple Access (NOMA) is a promising communication technique, which will satisfy the performance requirements for fifth-generation (5G) communications systems for both uplink and downlink scenarios [1]–[5]. Unlike conventional orthogonal multiple access (OMA) techniques including frequency division multiple access (FDMA), time division multiple access (TDMA), code division multiple access (CDMA) and orthogonal frequency division multiple access (OFDMA), that serve a single user in each orthogonal resource block, the NOMA can increase the number of users, improve spectrum efficiency, ensure massive connectivity, high performance, and low latency [6]–[11]. In downlink NOMA scenarios, all the individual information signals are superimposed on a single signal transmitted by the base station (BS) to the equipment users. For the decoding processes, most research works consider using successive interference cancellation (SIC) techniques in receiving devices to separate signals in the power domain

The associate editor coordinating the review of this manuscript and approving it for publication was Chen Chen[ID].

for each user [12]–[14]. Studies in the literature indicate that a key parameter for good NOMA performance is the correct power allocation per user [4], [15]. This performance can be measured based on the bit or symbol error rate (SER or BER); therefore, having exact expressions for these error rates is very significant since it will facilitate the design of the power allocation. Thus, some works can be found in the literature that aim to obtain closed-form BER expressions for different numbers of users and types of digital modulations [16], [17].

On the other hand, the classical Orthogonal Frequency Division Multiplexing (OFDM) is a multi-carrier waveform designed to deal with multipath reception problems such as inter-symbol interference. Mainly because OFDM presents a good performance and has a fairly simple implementation using the fast Fourier transform, this waveform is used in many modern communications systems, including the fifth-generation (5G) of mobile communication systems [18], [19]. However, this waveform has some disadvantages, such as high out-of-band emission (OOBE) and its high peak-to-average power ratio (PAPR) [20], [21]. This high PAPR is due to its multi-carrier nature and can generate non-linear distortions in the OFDM signal when it passes

through a non-linear High Power Amplifier (HPA) [22]. As a result of these non-linear distortions, a self-interference is produced, which degrades the system performance. Thus, studies that analyze the effect of HPA in OFDM are very important. In the literature, several works that explore the impact of HPA without memory can be found, for instance, the performance analysis in terms of SER, BER, and power spectral density [22]–[24], analysis of techniques for reducing the PAPR and linearization of HPA [25]–[27], implementation of PAPR reduction techniques [28]–[30] among others. However, although for wideband systems, memory effects should not be disregarded, very few papers analyzing this scenario can be found in the literature [31].

Considering the advantages of both NOMA and OFDM, in recent years, the scientific community has shown some interest in analyzing systems based on the joint use of these techniques. Some studies that can be found in the literature on NOMA-OFDM systems include: performance analysis in terms of BER [32], a proposal of methodologies for the decoding of the superimposed signals and power allocation [15], [33], analysis of channel estimation effects, and channel quantization in terms of BER [34], [35], energy efficiency analysis versus bandwidth spectrum efficiency [36], performance analysis considering index modulation techniques [37], [38] among others. However, to the best of the authors' knowledge, there are very few works that study the performance of NOMA-OFDM systems in the presence of HPAs. For instance, in [39] the analysis of the non-linear distortion effects associated with HPAs is performed. In [40] a design of a receiver to deal with non-linear distortions is presented. In [41] show an evaluation of the performance of the NOMA scheme in terms of outage probability and BER. Finally, in [42], a precoding technique is proposed to decrease the high PAPR and carrier frequency offset effects. It is important to highlight that, although some applications that will work over 5G mobile systems will require wide bandwidth, none of these studies consider the memory effects of the HPAs. Considering the above discussion, this paper aims to develop analytical expressions to analyze the performance of a downlink NOMA-OFDM system with two users operating in the presence of an HPA with memory. These results are pretty helpful to approach the design problem of the power allocation of NOMA systems; without using expensive computer simulation resources. To the best of the authors' knowledge, this is the first article that addresses this scenario.

Compared to the previously published works, the main contributions of our work are summarized as follows:

- Compared with the memory-less model of the HPA considered in [39]–[42], we consider a memory non-linear model in this paper.
- In contrast to the works presented in [39], [40], [42], which shows BER results obtained using only computational simulations, we present closed-form BER expressions for a two-user downlink NOMA-OFDM system.

These expressions allow obtaining curves for different parameters of the system easily.

- We present a theoretical characterization of non-linear distortions generated by HPA with memory.

The rest of the article is organized as follows: In Section II, the NOMA-OFDM signal and the non-linear model with memory are presented. Section III presents the development of BER analytical expressions of a downlink NOMA-OFDM system. In Section IV are presented numerical results for a particular NOMA-OFDM system with specific non-linear parameters. Finally, conclusions are given in section V.

II. SYSTEM MODEL

This section will present the NOMA-OFDM model and the non-linearity with memory considered in this work. As mentioned above, even though there is a signal superimpose in NOMA systems, it is possible to recover information if there is a proper power allocation. Thus, if we consider that the power allocation coefficient for user i is β_i, the complex envelope of the OFDM signal for the i-th user is given by

$$x_i[n] = \frac{\sqrt{\beta_i P_s}}{N} \sum_{k=0}^{N-1} a_{i,k} e^{j\frac{2\pi kn}{N}}, \qquad (1)$$

with $a_{i,k}$ representing the symbols transmitted by the user i on the sub-carrier k, N is the total number of sub-carriers, and $\beta_i P_s$ is the power assigned to the user i where P_s represents the total power. In this work, it will be considered that the symbols $a_{i,k}$ have unit energy and are independent for different sub-carriers, that is,

$$E[a_{i,k_1} a_{i,k_2}^*] = \delta[k_1 - k_2], \qquad (2)$$

where $\delta[\cdot]$ represent the well-known Kronecker delta function.

A. NON-LINEAR MODEL WITH MEMORY

The Volterra series is a well-known model for non-linear behavior that has the ability to capture memory effects. However, due to the mathematical complexity involved in this model, various simplifies forms have been proposed. Some of these proposals are Wiener [43], Hammerstein, [44] and the memory polynomial model (MPM) [45], [46]. In this work, the MPM will be used mainly because it is more tractable analytically and has shown promising results in modeling non-linearities with memory.

According to the MPM, the relationship between the input signal and the output signal of the non-linear HPA with memory is given by [45]

$$y_i[n] = \sum_{d=0}^{D} \sum_{q=0}^{Q} \alpha_{(2d+1),q} x_i[n - B_q] \left| x_i[n - B_q] \right|^{2d}, \quad (3)$$

where $x_i[\cdot]$ is the complex envelope representation of the input signal, B_q is the value of the q-th delay, D is the order of the non-linearity, Q is the total number of delays and $\alpha_{(2d+1),q}$ is the complex coefficient of $(2d+1)$-th non-linear order for delay q.

B. NOMA TRANSMISSION WITH HPA

As previously explained, the NOMA signal to be transmitted corresponds to a superimpose of all the user signals. Thus, the signal transmitted by the BS in a NOMA-OFDM system with HPA is given by

$$y[n] = \sum_{i=1}^{M} y_i[n], \tag{4}$$

where M is the total number of users and $y_i[n]$ is defined in (3). Using (3) in (4) gives

$$y[n] = \sum_{i=1}^{M} \sum_{d=0}^{D} \sum_{q=0}^{Q} \alpha_{(2d+1),q} x_i[n - B_q] \big| x_i[n - B_q] \big|^{2d}. \tag{5}$$

III. BER OF NOMA-OFDM

A. DECISION VARIABLE

In this work it is considered that the transmitted symbol is recovered using a matched filter receiver, in this way, the received symbol by the user m on the sub-carrier k, $\hat{a}_{m,k}$, is defined as

$$\hat{a}_{m,k} = h_m \sum_{n=0}^{N-1} y[n] e^{-j\frac{2\pi kn}{N}} + n_k, \tag{6}$$

where h_m represents the complex channel coefficients between BS and user m. Still in (6), n_k is related to the additive white Gaussian noise in the k-th sub-carrier, and it is considered that this noise is a random variable with zero mean and mean power P_n. Considering (5), the expression in (6) can be rewritten as

$$\hat{a}_{m,k} = h_m \sum_{n=0}^{N-1} \sum_{i=1}^{M} \sum_{d=0}^{D} \sum_{q=0}^{Q} \alpha_{(2d+1),q}$$
$$\times x_i[n - B_q] \big| x_i[n - B_q] \big|^{2d} e^{-j\frac{2\pi kn}{N}} + n_k. \tag{7}$$

Using the time-shift property in (7) gives

$$\hat{a}_{m,k} = h_m \sum_{n=0}^{N-1} \sum_{i=1}^{M} \sum_{d=0}^{D} \sum_{q=0}^{Q} \alpha_{(2d+1),q} \, x_i[n] \big| x_i[n] \big|^{2d}$$
$$\times e^{-j\frac{2\pi k(n+B_q)}{N}} + n_k. \tag{8}$$

Separating the symbol corresponding to the m-th user, we have that

$$\hat{a}_{m,k} = h_m \Gamma_{m,k} + h_m \sum_{\substack{i=1 \\ i \neq m}}^{M} \Gamma_{i,k} + n_k, \tag{9}$$

where

$$\Gamma_{i,k} = \sum_{n=0}^{N-1} \sum_{d=0}^{D} \sum_{q=0}^{Q} \alpha_{2d+1,q} x_i[n] \big| x_i[n] \big|^{2d} e^{-j\frac{2\pi k(n+B_q)}{N}}. \tag{10}$$

In general, a third-order non-linear model is capable of capturing all the information about the HPA distortions. Thus,

considering a third-order model (this is $D = 1$) and performing the summation in d, (10) can be rewritten as

$$\Gamma_{i,k} = \sum_{n=0}^{N-1} \sum_{q=0}^{Q} \alpha_{1,q} x_i[n] e^{-j\frac{2\pi k(n+B_q)}{N}}$$
$$+ \sum_{n=0}^{N-1} \sum_{q=0}^{Q} \alpha_{3,q} x_i[n] \big| x_i[n] \big|^2 e^{-j\frac{2\pi k(n+B_q)}{N}}. \tag{11}$$

Defining

$$A_{j,k} = \sum_{q=1}^{Q} \alpha_{j,q} e^{-j\frac{2\pi kB_q}{N}}, \tag{12}$$

it follows that

$$\Gamma_{i,k} = A_{1,k} \sum_{n=0}^{N-1} x_i[n] e^{-j\frac{2\pi kn}{N}}$$
$$+ A_{3,k} \sum_{n=0}^{N-1} x_i[n] \big| x_i[n] \big|^2 e^{-j\frac{2\pi kn}{N}}. \tag{13}$$

Using the definition of $x_i[n]$ given in (1) and considering that $\gamma_{i,n} = |x_i[n]|^2$, we can rewrite (13) as

$$\Gamma_{i,k} = A_{1,k} \sum_{n=0}^{N-1} \frac{\sqrt{\beta_i P_s}}{N} \sum_{k_1=0}^{N-1} a_{i,k_1} e^{j\frac{2\pi k_1 n}{N}} e^{-j\frac{2\pi kn}{N}}$$
$$+ A_{3,k} \sum_{n=0}^{N-1} \frac{\sqrt{\beta_i P_s}}{N} \sum_{k_1=0}^{N-1} a_{i,k_1} e^{j\frac{2\pi k_1 n}{N}} \gamma_{i,n} e^{-j\frac{2\pi kn}{N}}, \tag{14}$$

Separating the useful part of the information (i.e. $k_1 = k$), follows that

$$\Gamma_{i,k} = A_{1,k} \sqrt{\beta_i P_s} a_{i,k} + A_{3,k} \frac{\sqrt{\beta_i P_s}}{N} a_{i,k} \sum_{n=0}^{N-1} \gamma_{i,n}$$
$$+ A_{3,k} \frac{\sqrt{\beta_i P_s}}{N} \sum_{\substack{k_1=0 \\ k_1 \neq k}}^{N} a_{1,k_1} \sum_{n=0}^{N-1} \gamma_{i,n} e^{-j\frac{2\pi n(k-k_1)}{N}}. \tag{15}$$

After some mathematical manipulations, finally we have that

$$\Gamma_{i,k} = a_{i,k} Z_{i,k} + b_{i,k}, \tag{16}$$

where $Z_{i,k}$ is a constant given by

$$Z_{i,k} = \sqrt{\beta_i P_s} \left(A_{1,k} + A_{3,k} \frac{\beta_i P_s}{N} \right) \tag{17}$$

and

$$b_{i,k} = \frac{\sqrt{\beta_i P_s} A_{3,k}}{N} \sum_{\substack{k_1=0 \\ k_1 \neq k}}^{N} a_{i,k_1} \sum_{n=0}^{N-1} \gamma_{i,n} e^{-j\frac{2\pi n(k-k_1)}{N}}. \tag{18}$$

Note that, for obtaining (17) was used that

$$\sum_{n=0}^{N-1} \gamma_{i,n} = \sum_{n=0}^{N-1} |x_{i,n}|^2 = \beta_i P_s. \tag{19}$$

At this point, it is good to highlight that expression in (16) corresponds to the result of the well-known Bussgang theorem, which states that the non-linear system output is decoupled into two parts: A complex scaled version of the input signal and an additive non-linear noise. This non-linear noise can be considered Gaussian when the number of sub-carriers is relatively high, (i.e., greater than 16) [47].

Using (16) in (9) and realizing that $\Gamma_m = \Gamma_i$ for $i = m$, the received symbol is given by

$$\hat{a}_{m,k} = h_m\left(a_{m,k}Z_{m,k} + b_{m,k} + \sum_{\substack{i=1 \\ i\neq m}}^{M}\left[a_{i,k}Z_{i,k} + b_{i,k}\right]\right) + n_k \tag{20}$$

or

$$\hat{a}_{m,k} = h_m a_{m,k}Z_{m,k} + h_m \sum_{\substack{i=1 \\ i\neq m}}^{M} a_{i,k}Z_{i,k} + h_m \sum_{i=1}^{M} b_{i,k} + n_k. \tag{21}$$

Assuming that the receiver has perfect knowledge of the channel, the decision variable is defined as

$$D_{m,k} = \frac{\hat{a}_{m,k}}{h_m} = a_{m,k}Z_{m,k} + \sum_{\substack{i=1 \\ i\neq m}}^{M} a_{i,k}Z_{i,k} + N_{m,k}, \tag{22}$$

where the first term corresponds to the desire symbol, the second term is the inter-user interference and the third term represents the total noise given by

$$N_{m,k} = \sum_{i=1}^{M} b_{i,k} + \frac{n_k}{h_m}. \tag{23}$$

Considering the statistical properties of $b_{i,k}$ and n_k, it can be concluded that $N_{m,k}$ is a Gaussian random variable of zero mean and variance defined as

$$\sigma_{N_{m,k}}^2 = \sum_{i=1}^{M} \sigma_{b_{i,k}}^2 + \frac{P_n}{|h_m|^2} \tag{24}$$

where $\sigma_{b_{i,k}}^2$ represent the non-linear noise variance of user i given by

$$\sigma_{b_{i,k}}^2 = \frac{(\beta_i P_s)^3 |A_{3,k}|^2 (N-1)(3N-2)}{N^4}. \tag{25}$$

Details for the derivation of $\sigma_{b_{i,k}}^2$ are presented in Appendix.

B. EXACT BER EXPRESSIONS
Exact BER expressions can be obtained using the definition of the decision variable introduced in (22) and the statistical characteristics of the total noise presented above. However, these expressions depend on both the number of users and the modulation to be used. To facilitate the following analysis, we will consider a NOMA-OFDM system with two users using Q-PSK modulation. In this case, the expression presented in (22) allows to define the decision variables of the two users:

$$D_{1,k} = a_{1,k}Z_{1,k} + a_{2,k}Z_{2,k} + N_{1,k} \tag{26}$$
$$D_{2,k} = a_{2,k}Z_{2,k} + a_{1,k}Z_{1,k} + N_{2,k} \tag{27}$$

where

$$\sigma_{N_{m,k}}^2 = \sigma_{b_{1,k}}^2 + \sigma_{b_{2,k}}^2 + \frac{P_n}{|h_m|^2}; \quad m = \{1,2\}. \tag{28}$$

The decision process of user 1 is performed using

$$\hat{a}_{1,k} = \arg\min_{a_{1,k}\in\mathcal{A}_1} \left|D_{1,k} - a_{1,k}Z_{1,k}\right|^2, \tag{29}$$

where $\hat{a}_{1,k}$ represents the estimated symbol and $\mathcal{A}_1$ represents the alphabet of the user 1 constellation. In accordance with the theoretical analysis presented in [16], the probability of error of user 1 can be calculated using (30), as shown at the bottom of the page, where

$$d_1 = \sqrt{2}|Z_{2,k}|\cos\left[\frac{\pi}{4} + \angle\left(\frac{Z_{2,k}}{Z_{1,k}}\right)\right] \tag{31}$$

and

$$d_2 = \sqrt{2}|Z_{2,k}|\sin\left[\frac{\pi}{4} + \angle\left(\frac{Z_{2,k}}{Z_{1,k}}\right)\right]. \tag{32}$$

For the decoding process of user 2, the SIC is used. Firstly an estimate of $a_{1,k}$ is obtained using

$$\tilde{a}_{1,k} = \arg\min_{a_{1,k}\in\mathcal{A}_1} \left|D_{2,k} - a_{1,k}Z_{1,k}\right|^2. \tag{33}$$

Then the information corresponding to user 1 is subtracted from the decision variable, and a procedure similar to (29) is performed, that is,

$$\hat{a}_{2,k} = \arg\min_{a_{2,k}\in\mathcal{A}_2} \left|\tilde{D}_{2,k} - a_{2,k}Z_{2,k}\right|^2, \tag{34}$$

where $\hat{a}_{2,k}$ represents the estimated symbol, $\mathcal{A}_2$ represents the alphabet of the user 2 and

$$\tilde{D}_{2,k} = a_{2,k}Z_{2,k} + (a_{1,k} - \tilde{a}_{1,k})Z_{1,k} + N_{2,k}. \tag{35}$$

If the SIC process is performed perfectly (i.e. $a_{1,k} = \tilde{a}_{1,k}$) the BER is computed using

$$\rho_{2,k}^{PSIC} = Q\left(\sqrt{\frac{|Z_{2,k}|^2}{\sigma_{b_{1,k}}^2 + \sigma_{b_{2,k}}^2 + \frac{P_n}{|h_2|^2}}}\right). \tag{36}$$

$$\rho_{1,k} = \frac{1}{4}\left[Q\left(\frac{|Z_{1,k}| - d_1}{\sigma_{N_{1,k}}}\right) + Q\left(\frac{|Z_{1,k}| - d_2}{\sigma_{N_{1,k}}}\right) + Q\left(\frac{|Z_{1,k}| + d_1}{\sigma_{N_{1,k}}}\right) + Q\left(\frac{|Z_{1,k}| + d_2}{\sigma_{N_{1,k}}}\right)\right] \tag{30}$$

On the other hand, if the SIC process was not performed correctly, following the methodology presented in [16] the BER of user 2 is given by (37), as shown at the bottom of the page.

Finally, the average BER for either of the two users is calculated using

$$P_m = \frac{1}{N} \sum_{k=0}^{N} \rho_{m,k}. \tag{38}$$

IV. NUMERICAL RESULTS

In this section, the exact BER expressions of a NOMA-OFDM two-user system using Q-PSK presented in (30) and (37) are used to obtain numerical results. In addition, in order to validate these expressions, the same results are obtained but using Monte Carlo simulations. As can be seen in Figs. 1 to 6, all the theoretical results (solid lines) have a good agreement with the simulation results (dotted lines). All these results were obtained considering that both users use 32 sub-carriers ($N = 32$). The non-linear effect were analyzed based on the MPM's specific coefficients and the input Back-Off (IBO) defined as the ratio between the amplifier input saturation and the average transmitted power. The coefficients for the non-linear model with memory correspond to a sparse delay model [48] and are listed in Table 1.

FIGURE 1. Theoretical and simulated BER results for a NOMA-OFDM system with non-linear HPA with memory for two users, using Q-PSK, $N \; \mathcal{D} \; 32$, IBO = 15dB, SNR_1 = 12dB and different SNR_2 values.

Fig. 1 shows the BER results for user 1 and user 2 (for both with and without perfect SIC). Here it was considered that the signal-to-noise ratio of user 1 and the IBO are 12 dB and

TABLE 1. HPA polynomial memory delays and coefficients (Sparse delay).

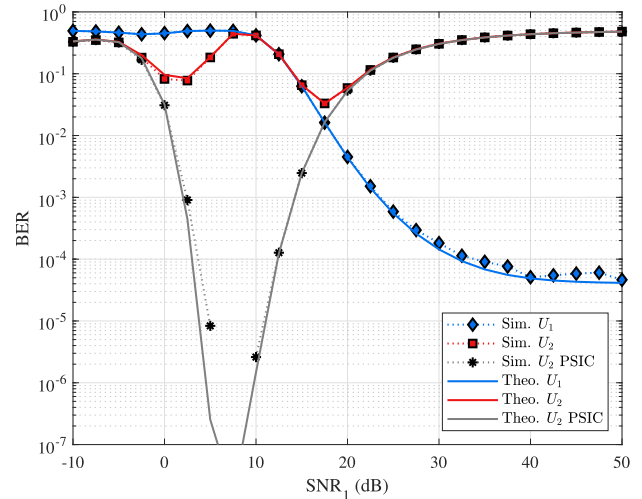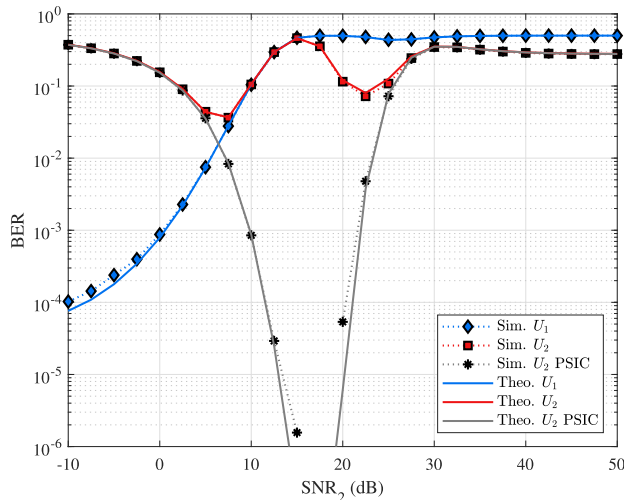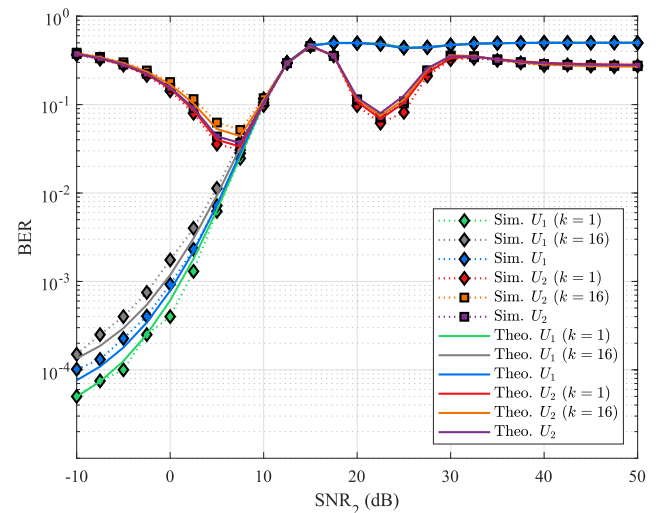| Delay	Coefficients Memory polynomial	
$B_0 = 0$	$\alpha_{1,0} = 0.9800 - 0.3000i$	$\alpha_{3,0} = -0.3000 + 0.4200i$
$B_1 = 10$	$\alpha_{1,1} = 0.0600 + 0.0300i$	$\alpha_{3,1} = -0.0200 + 0.0500i$
$B_2 = 50$	$\alpha_{1,2} = -0.0100 + 0.0200i$	$\alpha_{3,2} = 0.0200 - 0.0100i$
$B_3 = 100$	$\alpha_{1,3} = 0.0200 + 0.0800i$	$\alpha_{3,3} = -0.0100 + 0.0800i$

FIGURE 2. Theoretical and simulated BER results for a NOMA-OFDM system with non-linear HPA with memory for two users, using Q-PSK, $N = 32$, IBO = 15dB, SNR_2 = 12dB and different SNR_1 values.

FIGURE 3. BER results for user 1 on different sub-carriers using Q-PSK, $N = 32$, IBO = 15dB, SNR_1 = 12dB and different SNR_2 values.

15 dB respectively (i.e. SNR_1 = 15 dB and IBO = 15 dB). As expected, large values of the signal-to-noise ratio of user 2 (SNR_2) generate a BER degradation of user 1. Due to this

$$\rho_{2,k} = \frac{1}{4}\left[4Q\left(\frac{|Z_{2,k}|}{\sigma_{N_{2,k}}}\right) - Q\left(\frac{|Z_{1,k}| + d_1}{\sigma_{N_{2,k}}}\right) - Q\left(\frac{|Z_{1,k}| + d_2}{\sigma_{N_{2,k}}}\right) + Q\left(\frac{2|Z_{1,k}| + d_1}{\sigma_{N_{2,k}}}\right) + Q\left(\frac{2|Z_{1,k}| + d_2}{\sigma_{N_{2,k}}}\right) \right.$$
$$\left. + Q\left(\frac{|Z_{1,k}| - d_1}{\sigma_{N_{2,k}}}\right) + Q\left(\frac{|Z_{1,k}| - d_2}{\sigma_{N_{2,k}}}\right) - Q\left(\frac{2|Z_{1,k}| - d_1}{\sigma_{N_{2,k}}}\right) - Q\left(\frac{2|Z_{1,k}| - d_2}{\sigma_{N_{2,k}}}\right) \right] \tag{37}$$

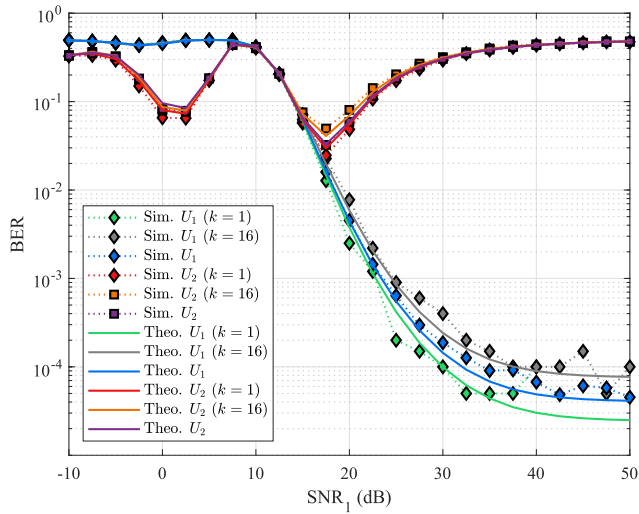**FIGURE 4.** BER results for user 2 on different sub-carriers using Q-PSK, $N = 32$, IBO = 15dB, SNR_2 = 12dB and different SNR_1 values.

FIGURE 5. Theoretical and simulated BER results for user 1 with different IBO values.

edge and center sub-carriers. As can be seen in these figures, there are only substantial differences between the sub-carriers for small values of SNR_2 or high values of SNR_1.

Figs. 5 and 6 show the influence of IBO on the performance of OFDM-NOMA systems. For example, in Fig. 5, we can observe the BER of user 1 for different values of IBO. This figure shows that the further away from its linear region the HPA operates (i.e., a high IBO), the worse the system performance. Fig. 6 shows the same result but for user 2. For comparison purposes, Figs. 5 and 6 show the results presented in [16] when a linear HPA is considered.

V. CONCLUSION
The main contribution of this paper is the development of analytical expressions of the BER in NOMA-OFDM systems operating in the presence of high-power amplifiers. Specifically, we develop exact BER expressions for a two-user downlink system using NOMA-OFDM. Unlike some works found in the literature, this paper considers a non-linear model capable of capturing the memory effects of the high-power amplifier. The numerical results obtained using these analytical expressions were validated by simulation results and showed that the non-linear distortions seriously degrade the performance of the systems.

APPENDIX
STATISTICAL CHARACTERIZATION OF THE NON-LINEAR NOISE OF THE *i*-TH USER
The mathematical expression of the non-linear noise presented in (18) can be rewrite as

$$b_{i,k} = \frac{\sqrt{\beta_i P_s} A_{3,k}}{N} \sum_{\substack{k_1=0 \\ k_1 \neq k}}^{N-1} B_{k_1}^i, \qquad (39)$$
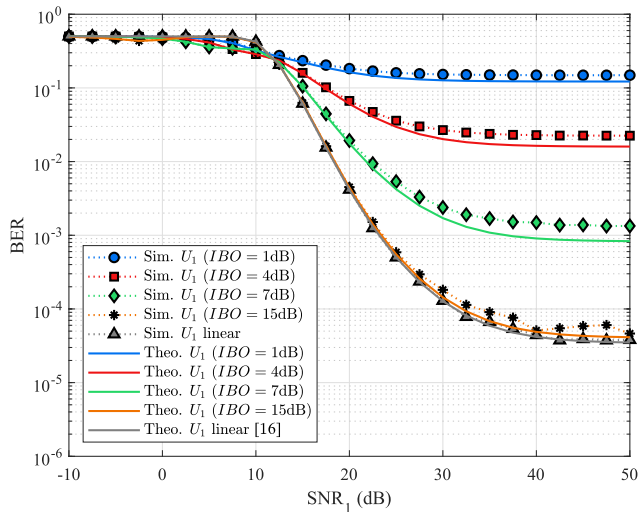

FIGURE 6. Theoretical and simulated BER results for user 2 with different IBO values.

degradation, the SIC process is performed imperfectly and therefore also generates a degradation in the BER of user 2. Fig. 2 also shows the BER results for users 1 and 2, but this time the signal-to-noise ratio of user 2 is set to 12 dB (SNR_2 = 12dB). As can be seen in this figure, for large values of SNR_1, there is a non-linear floor in the BER of user 1, mainly generated by the non-linear noise of the HPA with memory. Furthermore, this figure confirms that large values of SNR_1 lead to a degradation in user 2 performance.

Note that Figs. 1 and 2 show that despite a perfect SIC process, the BER of user 2 degrades significantly for high SNR_1 or SNR_2, due to the presence of the non-linear noise caused by the HPA.

In order to analyze the effect of non-linear distortions with memory on each sub-carrier, Figs. 3 and 4, in addition to presenting the average BER curve, present BER curves for the
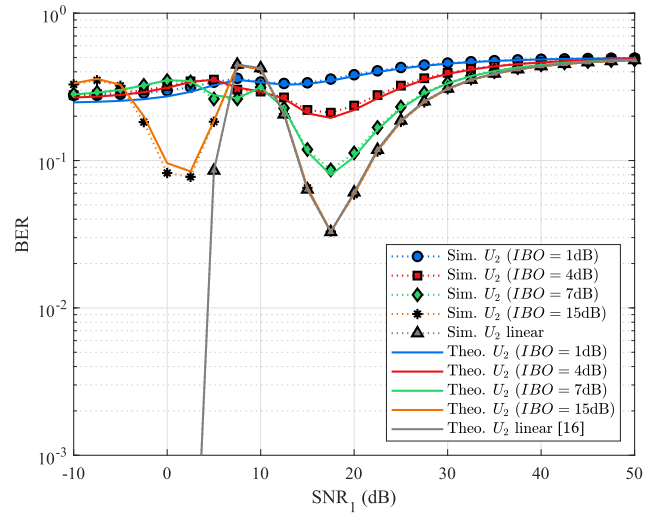
$$R_{k_1,k_2}^i = \frac{(\beta_i P_s)^2}{N^4} \sum_{n=0}^{N-1} \sum_{m=0}^{N-1} \sum_{\ell_1=0}^{N-1} \sum_{\ell_2=0}^{N-1} \sum_{\ell_3=0}^{N-1} \sum_{\ell_4=0}^{N-1} M_{a_i} e^{-j\frac{2\pi[n(k-k_1)-m(k-k_2)]}{N}} e^{j\frac{2\pi[n(\ell_1-\ell_2)+m(\ell_3-\ell_4)]}{N}} \tag{45}$$

where

$$B_{k_1}^i = \sum_{n=0}^{N-1} a_{i,k_1} \gamma_{i,n} e^{-j\frac{2\pi n(k-k_1)}{N}}. \tag{40}$$

Because the mean of $b_{i,k}$ is zero, its variance is given by

$$\sigma_{b_{i,k}}^2 = \frac{\beta_i P_s |A_{3,k}|^3}{N^2} \sum_{\substack{k_1=0 \\ k_1 \neq k}}^{N-1} \sum_{\substack{k_2=0 \\ k_2 \neq k}}^{N-1} R_{k_1,k_2}^i \tag{41}$$

with

$$R_{k_1,k_2}^i = E[B_{k_1}^i B_{k_2}^{i*}] \tag{42}$$

or, considering (40),

$$R_{k_1,k_2}^i = \sum_{n=0}^{N-1} \sum_{m=0}^{N-1} E[a_{i,k_1} a_{i,k_2}^* \gamma_{i,n} \gamma_{i,m}] e^{-j\frac{2\pi[n(k-k_1)-m(k-k_2)]}{N}}. \tag{43}$$

Recalling the definition of $\gamma_{i,n}$ given by

$$\gamma_{i,n} = |x_i[n]|^2 = \frac{\beta_i P_s}{N^2} \sum_{\ell_1=0}^{N-1} \sum_{\ell_2=0}^{N-1} a_{i,\ell_1} a_{i,\ell_2}^* e^{j\frac{2\pi n(\ell_1-\ell_2)}{N}}, \tag{44}$$

the expression of R_{k_1,k_2}^i can be rewrite as in (45), as shown at the top of the page, where

$$M_{a_i} = E[a_{i,k_1} a_{i,k_2}^* a_{i,\ell_1} a_{i,\ell_2}^* a_{i,\ell_3} a_{i,\ell_4}^*]. \tag{46}$$

To compute the expected value in (46) we can use the moment cumulants formula, thus,

$$\begin{aligned} M_{a_i} &= E[a_{i,k_1} a_{i,k_2}^*] E[a_{i,\ell_1} a_{i,\ell_2}^*] E[a_{i,\ell_3} a_{i,\ell_4}^*] \\ &+ E[a_{i,k_1} a_{i,k_2}^*] E[a_{i,\ell_1} a_{i,\ell_4}^*] E[a_{i,\ell_3} a_{i,\ell_2}^*] \\ &+ E[a_{i,k_1} a_{i,\ell_2}^*] E[a_{i,\ell_1} a_{i,\ell_4}^*] E[a_{i,\ell_3} a_{i,k_2}^*] \\ &+ E[a_{i,k_1} a_{i,\ell_2}^*] E[a_{i,\ell_1} a_{i,k_2}^*] E[a_{i,\ell_3} a_{i,\ell_4}^*] \\ &+ E[a_{i,k_1} a_{i,\ell_4}^*] E[a_{i,\ell_1} a_{i,\ell_2}^*] E[a_{i,\ell_3} a_{i,k_2}^*] \\ &+ E[a_{i,k_1} a_{i,\ell_4}^*] E[a_{i,\ell_1} a_{i,k_2}^*] E[a_{i,\ell_3} a_{i,\ell_2}^*] \end{aligned} \tag{47}$$

or considering the statistical properties of a_i (i.e. $E[a_{i,k_1} a_{i,k_2}^*] = \delta[k_1 - k_2]$)

$$\begin{aligned} M_{a_i} &= \delta[k_1 - k_2]\delta[\ell_1 - \ell_2]\delta[\ell_3 - \ell_4] \\ &+ \delta[k_1 - k_2]\delta[\ell_1 - \ell_4]\delta[\ell_3 - \ell_2] \\ &+ \delta[k_1 - \ell_2]\delta[\ell_1 - \ell_4]\delta[\ell_3 - k_2] \\ &+ \delta[k_1 - \ell_2]\delta[\ell_1 - k_2]\delta[\ell_3 - \ell_4] \\ &+ \delta[k_1 - \ell_4]\delta[\ell_1 - \ell_2]\delta[\ell_3 - k_2] \\ &+ \delta[k_1 - \ell_4]\delta[\ell_1 - k_2]\delta[\ell_3 - \ell_2]. \end{aligned} \tag{48}$$

Substituting the result of (48) in (45) and performing some algebra, it is obtained that

$$\begin{aligned} R_{k_1,k_2}^i = \frac{(\beta_i P_s)^2}{N^4} \Big[&N^4 \delta[k_1 - k_2]\delta[k_1 - k] + N^3 \delta[k_1 - k_2] \\ &+ 2N^3 \delta[k_1 - k] + 2N^2 \Big]. \end{aligned} \tag{49}$$

Finally, using (49) in (41) allows us to write that

$$\sigma_{b_{i,k}}^2 = \frac{(\beta_i P_s)^3 |A_{3,k}|^2 (N-1)(3N-2)}{N^4}. \tag{50}$$

REFERENCES

[1] T. A. Zewde and M. C. Gursoy, "NOMA-based energy-efficient wireless powered communications in 5G systems," in *Proc. IEEE 86th Veh. Technol. Conf. (VTC-Fall)*, Sep. 2017, pp. 1–5.

[2] Z. Ding, X. Lei, G. K. Karagiannidis, R. Schober, J. Yuan, and V. K. Bhargava, "A survey on non-orthogonal multiple access for 5G networks: Research challenges and future trends," *IEEE J. Sel. Areas Commun.*, vol. 35, no. 10, pp. 2181–2195, Oct. 2017.

[3] R.-A. Stoica, G. T. F. De Abreu, T. Hara, and K. Ishibashi, "Massively concurrent non-orthogonal multiple access for 5G networks and beyond," *IEEE Access*, vol. 7, pp. 82080–82100, 2019.

[4] A. Abrardo, M. Moretti, and F. Saggese, "Power and subcarrier allocation in 5G NOMA-FD systems," *IEEE Trans. Wireless Commun.*, vol. 19, no. 12, pp. 8246–8260, Dec. 2020.

[5] A. Agarwal, R. Chaurasiya, S. Rai, and A. K. Jagannatham, "Outage probability analysis for NOMA downlink and uplink communication systems with generalized fading channels," *IEEE Access*, vol. 8, pp. 220461–220481, 2020.

[6] G. Liu, Z. Wang, J. Hu, Z. Ding, and P. Fan, "Cooperative NOMA broadcasting/multicasting for low-latency and high-reliability 5G cellular V2X communications," *IEEE Internet Things J.*, vol. 6, no. 5, pp. 7828–7838, Oct. 2019.

[7] K. F. Shamna, C. I. Siyad, S. Tamilselven, and M. K. Manoj, "Deep learning aided NOMA for user fairness in 5G," in *Proc. 7th Int. Conf. Smart Struct. Syst. (ICSSS)*, Jul. 2020, pp. 1–6.

[8] K. Selvam and K. Kumar, "Energy and spectrum efficiency trade-off of non-orthogonal multiple access (NOMA) over OFDMA for machine-to-machine communication," in *Proc. 5th Int. Conf. Sci. Technol. Eng. Math. (ICONSTEM)*, Mar. 2019, pp. 523–528.

[9] X. Liu, Y. Liu, X. Wang, and H. Lin, "Highly efficient 3-D resource allocation techniques in 5G for NOMA-enabled massive MIMO and relaying systems," *IEEE J. Sel. Areas Commun.*, vol. 35, no. 12, pp. 2785–2797, Dec. 2017.

[10] Y. Zhang, J. Ge, and E. Serpedin, "Performance analysis of a 5G energy-constrained downlink relaying network with non-orthogonal multiple access," *IEEE Trans. Wireless Commun.*, vol. 16, no. 12, pp. 8333–8346, Dec. 2017.

[11] Y. Liu, Z. Qin, M. Elkashlan, Z. Ding, A. Nallanathan, and L. Hanzo, "Nonorthogonal multiple access for 5G and beyond," *Proc. IEEE*, vol. 105, no. 12, pp. 2347–2381, Dec. 2017.

[12] J. Zhao, X. Yue, S. Kang, and W. Tang, "Joint effects of imperfect CSI and SIC on NOMA based satellite-terrestrial systems," *IEEE Access*, vol. 9, pp. 12545–12554, 2021.

[13] L. Chuan, C. Qing, and L. Xianxu, "Uplink NOMA signal transmission with convolutional neural networks approach," *J. Syst. Eng. Electron.*, vol. 31, no. 5, pp. 890–898, Oct. 2020.

[14] K. Jiang, T. Jing, Y. Huo, F. Zhang, and Z. Li, "SIC-based secrecy performance in uplink NOMA multi-eavesdropper wiretap channels," *IEEE Access*, vol. 6, pp. 19664–19680, 2018.

[15] G. Wang, Y. Shao, L.-K. Chen, and J. Zhao, "Subcarrier and power allocation in OFDM-NOMA VLC systems," *IEEE Photon. Technol. Lett.*, vol. 33, no. 4, pp. 189–192, Feb. 15, 2021.

[16] X. Wang, F. Labeau, and L. Mei, "Closed-form BER expressions of QPSK constellation for uplink non-orthogonal multiple access," *IEEE Commun. Lett.*, vol. 21, no. 10, pp. 2242–2245, Oct. 2017.

[17] S. Baig, U. Ali, H. M. Asif, A. A. Khan, and S. Mumtaz, "Closed-form BER expression for Fourier and wavelet transform-based pulse-shaped data in downlink NOMA," *IEEE Commun. Lett.*, vol. 23, no. 4, pp. 592–595, Apr. 2019.

[18] *IMT Vision—Framework and Overall Objectives of the Future Development of IMT for 2020 and Beyond*, document Recommendation ITU-R M.2083-0 (09/2015), 2015.

[19] *Requirements of IMT-2020 Network*, document Draft Recommendation Y.IMT2020-reqts, 2020.

[20] Z. E. Ankarali, A. Sahin, and H. Arslan, "Joint time-frequency alignment for PAPR and OOBE suppression of OFDM-based waveforms," *IEEE Commun. Lett.*, vol. 21, no. 12, pp. 2586–2589, Dec. 2017.

[21] A. M. Rateb and M. Labana, "An optimal low complexity PAPR reduction technique for next generation OFDM systems," *IEEE Access*, vol. 7, pp. 16406–16420, 2019.

[22] H. Shaiek, R. Zayani, Y. Medjahdi, and D. Roviras, "Analytical analysis of SER for beyond 5G post-OFDM waveforms in presence of high power amplifiers," *IEEE Access*, vol. 7, pp. 29441–29452, 2019.

[23] A. Lipovac and A. Mihaljevic, "BER based OFDM PAPR estimation," in *Proc. 26th Int. Conf. Softw., Telecommun. Comput. Netw. (SoftCOM)*, Sep. 2018, pp. 1–6.

[24] P. Aggarwal, A. Agarwal, and V. A. Bohara, "On the spectral content of the nonlinearly amplified carrier aggregated OFDM system," in *Proc. IEEE Wireless Commun. Netw. Conf. (WCNC)*, Apr. 2018, pp. 1–5.

[25] R. Zayani, H. Shaïek, and D. Roviras, "Ping-pong joint optimization of PAPR reduction and HPA linearization in OFDM systems," *IEEE Trans. Broadcast.*, vol. 65, no. 2, pp. 308–315, Jun. 2019.

[26] S. Thota, Y. Kamatham, and C. S. Paidimarry, "Analysis of hybrid PAPR reduction methods of OFDM signal for HPA models in wireless communications," *IEEE Access*, vol. 8, pp. 22780–22791, 2020.

[27] Z. Liu, X. Hu, K. Han, S. Zhang, L. Sun, L. Xu, W. Wang, and F. M. Ghannouchi, "Low-complexity PAPR reduction method for OFDM systems based on real-valued neural networks," *IEEE Wireless Commun. Lett.*, vol. 9, no. 11, pp. 1840–1844, Nov. 2020.

[28] Y. Kamatham and S. Pollamoni, "Implementation of OFDM system with companding for PAPR reduction using NI-USRP and LabVIEW," in *Proc. IEEE Int. WIE Conf. Electr. Comput. Eng. (WIECON-ECE)*, Nov. 2019, pp. 1–4.

[29] H. Iqbal and S. A. Khan, "Selective mapping: Implementation of PAPR reduction technique in OFDM on SDR platform," in *Proc. 24th Int. Conf. Autom. Comput. (ICAC)*, Sep. 2018, pp. 1–6.

[30] S. Gökceli, P. P. Campo, T. Levanen, J. Yli-Kaakinen, M. Turunen, M. Allén, T. Riihonen, A. Palin, M. Renfors, and M. Valkama, "SDR prototype for clipped and fast-convolution filtered OFDM for 5G new radio uplink," *IEEE Access*, vol. 8, pp. 89946–89963, 2020.

[31] H. Zhi-Yong, G. Jian-Hua, G. Shu-Jian, and W. Gang, "An improved look-up table predistortion technique for HPA with memory effects in OFDM systems," *IEEE Trans. Broadcast.*, vol. 52, no. 1, pp. 87–91, Mar. 2006.

[32] Y. Kabalci and M. Ali, "Downlink performance evaluation of NOMA systems based on different OFDM waveforms," in *Proc. 1st Global Power, Energy Commun. Conf. (GPECOM)*, Jun. 2019, pp. 106–111.

[33] H. Ren, Z. Wang, S. Han, J. Chen, C. Yu, C. Xu, and J. Yu, "Performance improvement of M-QAM OFDM-NOMA visible light communication systems," in *Proc. IEEE Global Commun. Conf. (GLOBECOM)*, Dec. 2018, pp. 1–6.

[34] J. Angjo, M. M. Tuncer, E. Akertek, H. Alakoca, M. Basaran, and L. Durak-Ata, "On the channel estimation performance of NOMA systems: Experimental implementation of real-time downlink NOMA-OFDM," in *Proc. IEEE Int. Black Sea Conf. Commun. Netw. (BlackSeaCom)*, May 2020, pp. 1–6.

[35] M. B. Balogun, F. Takawira, and O. O. Oyerinde, "Weighted least square based iterative channel estimation for uplink NOMA-OFDM systems," in *Proc. 13th Int. Conf. Signal Process. Commun. Syst. (ICSPCS)*, Dec. 2019, pp. 1–5.

[36] K. Selvam and K. Kumar, "Green point energy-efficient analysis of non-orthogonal multiple access (NOMA) over OFDMA," in *Proc. Int. Conf. Emerg. Trends Inf. Technol. Eng. (IC-ETITE)*, Feb. 2020, pp. 1–5.

[37] A. Tusha, S. Dogan, and H. Arslan, "A hybrid downlink NOMA with OFDM and OFDM-IM for beyond 5G wireless networks," *IEEE Signal Process. Lett.*, vol. 27, pp. 491–495, 2020.

[38] X. Chen, M. Wen, and S. Dang, "On the performance of cooperative OFDM-NOMA system with index modulation," *IEEE Wireless Commun. Lett.*, vol. 9, no. 9, pp. 1346–1350, Sep. 2020.

[39] J. Guerreiro, R. Dinis, P. Montezuma, and M. M. da Silva, "Non-linear effects in NOMA signals: Performance evaluation and receiver design," in *Proc. IEEE 90th Veh. Technol. Conf. (VTC-Fall)*, Sep. 2019, pp. 1–5.

[40] J. Guerreiro, R. Dinis, P. Montezuma, and M. Campos, "On the receiver design for nonlinear NOMA-OFDM systems," in *Proc. IEEE 91st Veh. Technol. Conf. (VTC-Spring)*, May 2020, pp. 1–6.

[41] O. B. H. Belkacem, M. L. Ammari, and R. Dinis, "Performance analysis of NOMA in 5G systems with HPA nonlinearities," *IEEE Access*, vol. 8, pp. 158327–158334, 2020.

[42] V. K. Trivedi, K. Ramadan, P. Kumar, M. I. Dessouky, and F. E. A. El-Samie, "Enhanced OFDM-NOMA for next generation wireless communication: A study of PAPR reduction and sensitivity to CFO and estimation errors," *AEU-Int. J. Electron. Commun.*, vol. 102, pp. 9–24, Apr. 2019.

[43] C. J. Clark, G. Chrisikos, M. S. Muha, A. A. Moulthrop, and C. P. Silva, "Time-domain envelope measurement technique with application to wideband power amplifier modeling," *IEEE Trans. Microw. Theory Techn.*, vol. 46, no. 12, pp. 2531–2540, Dec. 1998.

[44] T. Wang and J. Ilow, "Compensation of nonlinear distortions with memory effects in digital transmitters," in *Proc. 2nd Annu. Conf. Commun. Netw. Services Res.*, 2004, pp. 3–9.

[45] J. Kim and K. Konstantinou, "Digital predistortion of wideband signals based on power amplifier model with memory," *Electron. Lett.*, vol. 37, no. 23, pp. 1417–1418, Nov. 2001.

[46] L. Ding, G. T. Zhou, D. R. Morgan, Z. Ma, J. S. Kenney, J. Kim, and C. R. Giardina, "A robust digital baseband predistorter constructed using memory polynomials," *IEEE Trans. Commun.*, vol. 52, no. 1, pp. 159–165, Jan. 2004.

[47] T. Araujo and R. Dinis, "On the accuracy of the Gaussian approximation for the evaluation of nonlinear effects in OFDM signals," *IEEE Trans. Commun.*, vol. 60, no. 2, pp. 346–351, Feb. 2012.

[48] H. Ku and J. S. Kenney, "Behavioral modeling of nonlinear RF power amplifiers considering memory effects," *IEEE Trans. Microw. Theory Techn.*, vol. 51, no. 12, pp. 2495–2504, Dec. 2003.

ALEXANDER HILARIO-TACURI was born in Perú in, 1988. He received the degree in electronic engineering (telecommunications) from the Universidad Nacional de San Agustín de Arequipa (UNSA), Perú, in 2008, and the M.Sc. and Ph.D. degrees in electrical engineering from the Pontifícia Universidade Católica do Rio de Janeiro (PUC-Rio), Brazil, in 2010 and 2014, respectively. After Ph.D. graduation, he was a Senior Researcher with Engenho Company on Research and Development, where he was the Head of the Research Group. From March 2015 to December 2016 he was a Postdoctoral Fellow with the Department of Electrical Engineering, Pontifícia Universidade Católica do Rio Grande do Sul, Porto Alegre, Brazil. From August 2015 to November 2015, he was a Visiting Researcher with Stanford University. He returned to UNSA, in January 2017 and, since then, he has been a Professor with the Electronic Engineering Department. In 2018, while on a sabbatical leave, he was a Postdoctoral Fellow with the Department of Electrical Engineering, PUC-Rio, working in the University Center for Telecommunications Studies (CETUC). He has published many articles in national and international journals and conferences. His main research interests include 5G cellular networks, communication theory, satellite communications, estimation theory, digital transmission, and signal processing for communications.

JESUS MALDONADO (Student Member, IEEE) was born in Arequipa, Perú, in 1999. He is currently pursuing the bachelor's degree in electronic engineering with the National University of San Agustin of Arequipa, Arequipa, forming part of the top tenth of his class. His research interests include communication signal processing, telecommunications engineering, and control engineering.

HERNAN CHAMBI was born in Perú, in 1992. He is currently pursuing the degree in electronic engineering with the National University of San Agustín (UNSA), Arequipa, Perú. He is currently part of the top tenth of his career in electronic engineering in his last year. His current research interests include mobile communication systems, digital signal processing, automation, control engineering, and robotics.

• • •

MARIO REVOLLO was born in Bolivia, in 2000. He is currently pursuing the degree in electronic engineering with the National University of San Agustín (UNSA). He is currently a part of the top tenth in his school's ranking, being in the last year in the career of electronic engineering. His research interests include mobile communication systems, digital signal processing, and control engineering.